Available online at www.sciencedirect.com

ScienceDirect

journal homepage: www.elsevier.com/locate/he

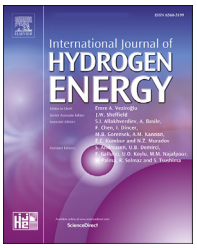

Simulation of a stabilised control strategy for PEM fuel cell and supercapacitor hybrid propulsion system for a city bus

W. Wu, J.S. Partridge*, R.W.G. Bucknall

Dept. of Mechanical Engineering, UCL, UK

ARTICLE INFO

Article history:
Received 7 June 2018
Received in revised form
21 August 2018
Accepted 1 September 2018
Available online 22 September 2018

Keywords:
Fuel cell
Supercapacitor
Hybrid propulsion
Energy management
Simulink

ABSTRACT

Fuel Cells (FC) are a clean energy source capable of powering a bus electrically with zero operating emissions. This research investigates the potential of FC and Supercapacitor (SC) hybrid buses for clean city transportation. To investigate the FC/SC hybridisation strategy, a scaled FC/SC hybrid drivetrain has been developed to provide the power system of a scaled bus model. The scaled model was developed as a MATLAB Simulink computer model and cross referenced against the constructed laboratory test rig for validation. A novel control strategy focusing on power balancing between the FC, the SC and the load has been developed and validated in the computer model. It has been demonstrated in both the test rig and computer simulation that the proposed control strategy is capable of maintaining a controlled and stable FC output while meeting different bus load regimes. The validated computer model can provide a reliably representative, convenient and low cost platform for further performance investigation and component optimisation of FC/SC hybrid drivetrains. The control strategy has also been demonstrated to be function as expected after scaling up the developed scaled model to a full scale model which can be used for simulation of practical bus performance.

Introduction

The harmful transportation derived emissions resulting from heavy traffic in a city not only contain greenhouse gases contributing to climate change, but can also affect human physical health and significantly affect large cities like London. The Transport for London (TfL) *Transport Emission Roadmap Report 2014* indicated that London's transport is a key contributor to several emission types [1,2]. Studies indicate that 21% of CO_2 emissions, 63% of NOx emissions and 52% of PM_{10} emissions result from transportation activity in London as a result of large scale transportation demands [3–5]. Within the public transportation sector, London buses are both the largest CO_2 emissions contributor from among all other London public transportation modes and the largest NO_X emissions contributor, accounting for 72% of all NO_X emissions from TfL operations [6].

The UK bus industry has been driving innovative technology in the quest for lower emissions and greater efficiency over the past decades. Significant progress has been made regarding "greener" bus development and the technology is

* *Corresponding author.*
E-mail address: julius.partridge.09@ucl.ac.uk (J.S. Partridge).
https://doi.org/10.1016/j.ijhydene.2018.09.004

Nomenclature

I_{fc_in}	Current output from the Fuel Cell
I_{fc_out}	Current output from the boost converter on the common busbar
I_{fc_ref}	Reference value for the boost converter current output on the common busbar
I_{load}	Current to/from the traction motor
I_{SC_in}	Current to/from the Supercapacitor
I_{SC_out}	Current to/from the Buck/Boost converter on the common busbar
V_{fc_in}	Voltage across the Fuel Cell
V_{fc_out}	Voltage across the Boost converter on the busbar
V_{load}	Voltage across the traction motor controller on the busbar
V_{SC_in}	Voltage across the supercapacitor
V_{SC_out}	Voltage across the Buck/Boost converter on the busbar

being distributed across the UK [7]. The development of a cleaner power source for buses can be summarised as being in two phases with 2020 as a key milestone. Before 2020, the mass implementation and distribution of well-developed diesel hybrid propulsion buses will offer relatively rapid payback in terms of emission reductions. After 2020, other technologies that offer further emission reduction over typical diesel hybrid buses will start to be deployed and evaluated as a longer term solution [8]. The mass deployment of diesel hybrid buses in London has shown significant payback in terms of improved fuel economy and reduced environmental impact from 2013 [9,10]. However, the diesel hybrid bus will eventually reach an emission reduction threshold because it is still diesel-based technology. TfL has been investigating other long term technological solutions and one of the more promising is Fuel Cell technology [11].

The Proton Exchange Membrane Fuel Cell (FC) offers a clean energy source with the main benefits of zero harmful emissions and relatively high efficiency at point of use. The FC uses hydrogen as fuel and generates electricity through an electrochemical process with water as a waste product [12]. However, the main barrier to FC powered buses is their high capital cost [13,14]. A FC powered bus costs approximately five times that of a conventional diesel bus with similar power output [14]. The high cost is mainly a consequence of the requirement of a large FC stack on-board and the low volume of component production for FC systems which impacts economies of scale [14]. Current FC bus systems still need improvement both technically and economically to overcome this barrier.

The work in this paper is a continuation of the research presented in Ref. [15]. In that work, a FC and Supercapacitor (SC) laboratory test rig has been constructed with the aim of developing and defining an optimised control strategy between the FC and the SC. A simple control strategy focused on keep the FC output stable and user controlled has been developed and tested on the laboratory test rig. It was determined that the stabilised FC output control strategy can significantly mitigate against and attenuate the potential stresses that would normally be applied on the FC and thereby extend the FC stack life and reduce the gross FC power and size requirement. Details of the laboratory test rig and control strategy development can be found in Refs. [15] and [16].

In much of the available literature on FC system simulations, a unidirectional boost converter was used to control the FC output because the FC losses vary with the output power of the FC [17]. Example of passive systems have been explored, such as [18–21], these use the SC as a means of damping the response rate of the FC to limit the transient power changes. However, they necessitate considerable variations to the FC output and require a large FC to cover the load power requirements. Since the focus of this research was to maintain a stable FC output, active control of the FC output through power electronic converters was required. Different control algorithms for FC output power control in a hybrid system have been developed in recent years. Kuo and Hsieh developed a relationship between the power balancing in their FC/battery hybrid system and the vehicle speed to control the FC output power [22]. However, owing to their active FC output control algorithm, the FCs are subject to significant power output variations due to the direct link to the load. A number of different control algorithm have been proposed in other literature to reduce FC variations. The work presented in Refs. [23–26] proposed a method of having a number of different pre-defined fixed output level controlled by the load demand to adjust the FC output power. This method can reduce FC variation, however, it has been observed that the FC output has to be constantly adjusted during large dynamic load operations and the FC could be involved in on-and-off operation during low power load operation. Work presented in Refs. [27–29] developed FC output control algorithms that are dependent on the SoC of the energy storage. The FC output power has been controlled by using the boost converter. Although this method of controlling FC output based on real time SoC adds flexibility in the system, the FC output was still subject to significant variations. In the work of [30] a FC/battery electrical system has been simulated in Simulink. The system offers significant mass and volume reduction when compared to a battery only system, however the strategy employs a simple on-off strategy for the FC and thus results in significant transient load changes of the FC. In the work of [31] the FC output was controlled at a number of predefined load states. This offered faster response times over previous strategies, however again required significant transient load changes for the FC. The research presented so far is concerned primarily with the algorithms used to share the power balance between different components. In addition, much work has been done on control strategies and their impacts on component sizing, hydrogen consumption and cost. In the work of [32–34] the cost and fuel consumption was considered [35,36], considered the fuel consumption and [37] considered the FC lifetime through optimisation of the balance of power, however, the details of the operation of the electrical system were not considered. The literature has highlighted a wide array of strategies used to control FC hybrid propulsion systems, however these mostly require significant transient responses to the FC output to meet the load power demands.

The work in this paper instead focuses on maintaining a stable FC output, thus reducing the stress on the FC from transient load changes and has been carried out from the perspective of the electrical system.

Although the laboratory test rig demonstrated the performance of the proposed FC hybrid system, it lacks configuration and sizing flexibility. This provides additional motivation for developing the system from a computational standpoint. Previous work on PEM Fuel Cell hybrid system modelling utilised control strategies that require a dynamic response from the FC, which could damage the FC. As a result, this work intends to simulate a different control strategy that is capable of keeping the FC output controlled and constant while meeting dynamic power demands. This focuses on the operation of the hybrid electric system and the balance of power between the constituent power sources to provide for the load power requirements whilst maintaining the bus voltage. This includes the modelling and control of the power electronic converters used to achieve this and the impact on the energy storage system during operation. The work builds upon the laboratory test rig detailed in Refs. [15,16] with a computational approach. A computer Simulink model has been developed to represent the same laboratory test rig. The purposes of modelling the FC/SC hybrid system are:

1. Development of the FC/SC hybrid system from a computational approach. The results obtained from the laboratory test rig will be used to validate the computer model ensuring the computer model is representative of the laboratory system.
2. Validation of the stabilised FC output control strategy under the same load conditions as the experiments carried out with the laboratory test rig. This will further verify the control strategy from a computational approach.
3. Provide a validated computer model to enable great flexibility for system modification and allow a wider scope during further investigation.
   - Enable more accessible, quicker and cheaper component modification and sizing.
   - Enable system performance evaluation and controller assessment with a much wider range of load conditions.
   - Enable system optimisation while encompassing a wider suite and range of system parameters.
   - Enable quick and easier comparison of different system configuration and component sizing.
   - Enable more accessible scaling of the system and enable evaluation of full scale models at the power level of a practical bus, opening up the possibility for system design on a practical scale.

System configuration

The system configuration of the computer model, shown in Fig. 1 utilises the same configuration as the laboratory test rig. The series hybrid configuration was selected to utilise the FC's high energy density and SC's high power density. The high energy density of the FC makes it more appropriate to work as a primary energy source that delivers a steady output power during operation. The high power density of a SC makes it suitable to satisfy any short transient power demands during operation. Their opposing characteristics in terms of energy/power density make them complementary when working together in a hybrid system. More detail on the development of the utilised hybrid configuration can be found in the laboratory test rig development paper [15].

The hybrid model is comprised of three sub-systems which are the FC system, SC system and the load system. The FC system consists of a FC, which is the energy and main power source of the hybrid system, and a boost converter, which enables voltage regulation for the FC output. The SC system consists of a SC, which allows energy harvesting, storage and release on demand in the system, and a buck/boost converter, which controls the SC charge and discharge. The load system consists of a variable resistor and a controlled power source which can be used to simulate different load conditions.

The FC/SC hybrid system can be operated in three modes. The three modes are expected to mirror the power requirement of typical city bus operation. In mode 1, the SC will be used to supplement the FC to provide a higher transient output which simulates bus acceleration, climbing of gradients or under heavy loading. In mode 2, the FC will both power the load and use excess power to charge the SC which simulates the bus operation when the FC is providing more power than the bus load requirement. In mode 3, the energy recaptured through regenerative braking will be used to charge the SC in conjunction with the FC output which simulates the bus engaging regenerative braking. Details of the operating modes and development of the laboratory system can be found in Ref. [15]. The control strategy implemented has been outlined in Ref. [15], where the hybrid system is managed through continually updating the reference current for the output of the SC buck/boost converter. This considers the difference in the load current requirements and the desired FC current output (both measured on the common bus) to determine the required reference value which requires a negligible calculation time.

System simulation

The three sub-systems will be replicated as computer models. Simulink has been selected as the simulation tool in order to align with the overarching project requirements and to facilitate the integration of existing models. Each sub-system in the computer model will be based on the components used in the laboratory test rig. The simulation results will be validated against the results obtained from the laboratory test rig. The individual sub-systems were first developed separately and then integrated to produce the hybrid system. The development of each individual component and system integration will be described in the following sections.

Fuel cell system simulation

The FC system consists of a FC and a boost converter. The simulation of the FC focused on the electrical characteristics of the proposed 8.5 kW FC described in the laboratory system. The PEMFC has a very high theoretical efficiency. This

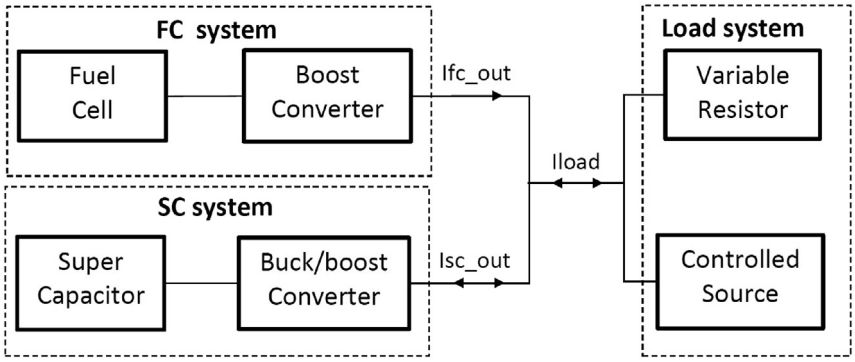

Fig. 1 – Overview of the system configuration of the computer model.

theoretical efficiency can be achieved only if all the Gibbs free energy (electrical work) has been fully utilised, however, there will always be energy losses during the process, in this case, voltage drops resulting from the work energy required to produce the electrical output. There are three main reasons for significant voltage loss for PEMFC: these are activation loss, ohmic loss and concentration loss. The voltage parameters can be mathematically represented in the computer model to represent the realistic output voltage of the FC. In MATLAB Simulink, a generic hydrogen fuel cell stack model can be modified to represent some of the more popular types of fuel cell stacks. The Simulink model calculates the three voltage losses based on the current output and assigns a calculated voltage by a mathematical method. Simulink was used to produce a polarisation curve through calculation using the parameters loaded from the data sheet. The data sheet of the laboratory FC has been imported to the Simulink generic FC model to simulate the same laboratory FC. The data sheet can be found in Ref. [38] with the values shown in Table 1.

In order to evaluate the FC across different power ranges, a DC electrical resistive load system has been developed for the FC. The resistive load for the laboratory FC evaluation test has been selected as ten parallel connected resistors (0.744Ω each). The resistances were selected to cover the whole power range of the FC and each resistor is controlled by a separate switch. The resistance values of the computer model resistors were set to match those of the laboratory system and the same experimental sequence for loading the FC was followed. The computer simulation results have been compared with the laboratory system results and are shown in Fig. 2.

Table 1 – Input parameters of the laboratory and Simulink model FC.

	Laboratory FC	Simulink FC
Number of cells	40	40
Nominal stack efficiency (%)	51	51
Operating temperature (oC)	50–60	60
Nominal fuel supply pressure (bar)	1.18	1.18
Nominal composition (%) [H_2 O_2]	99.995 21	99.99 21
Open circuit voltage (V)	36	36
Maximum operating point voltage (V)	26	26
Maximum operating point current (A)	350	330.8

As the FC current and voltage curves show, the FC output step responses are generally the same as the laboratory results. However, the voltages from the Simulink FC model are slightly higher than the corresponding results for the laboratory system and consequently affected the output current performance, particularly for the last few step changes. This is caused by the temperature stabilisation of the laboratory system. The FC stack needs to attain a certain temperature to achieve the optimised efficiency. It can be seen that the voltage increases over time during each step because of the increasing temperature. The FC temperature takes longer to reach the required level in the laboratory system while this is not a factor for the computer simulation. This will have less impact on the difference between laboratory system and Simulink model if the load change is not stepped.

As the FC characteristic curve show (Fig. 2), the FC output voltage drops as the power delivered increases. This reduction in terminal voltage may not be an issue for purely resistive loads, but could be a problem for motor loads. Motor controllers and motors are normally designed to operate within a reasonably narrow supply voltage range. As a result, the boost converter has been used to maintain a near steady output voltage for the motor. Four levels of resistive load (load 1 is 2.05 Ω, load 2 is 0.9669 Ω, load 3 is 0.6253 Ω, load 4 is 0.4681 Ω) have been applied to the FC and boost converter output as loads. The output current and voltage of the boost converter have been shown in Fig. 3.

For the input performance, the results from Simulink showed lower input current and higher input voltage when compared with the results from laboratory. It has been found there is a trend showing the results from laboratory approaches to the Simulink converter as the power increases. This is caused by the difference in FC output power being affected by the FC temperature. The laboratory FC takes longer to warm up to achieve the expected performance. For the output performance, the boost converter output current characteristic of the Simulink model is nearly identical to the laboratory result. The initial discrepancy was caused by the PID number being set to 0 at start up and it only occurs during start up as the internal capacitors in the boost converter charge. The boost converter output voltage of the Simulink model was maintained at 48 V, however, voltage drops are observed with the computer simulation whenever a load change occurs. This is caused by the PID controller taking a

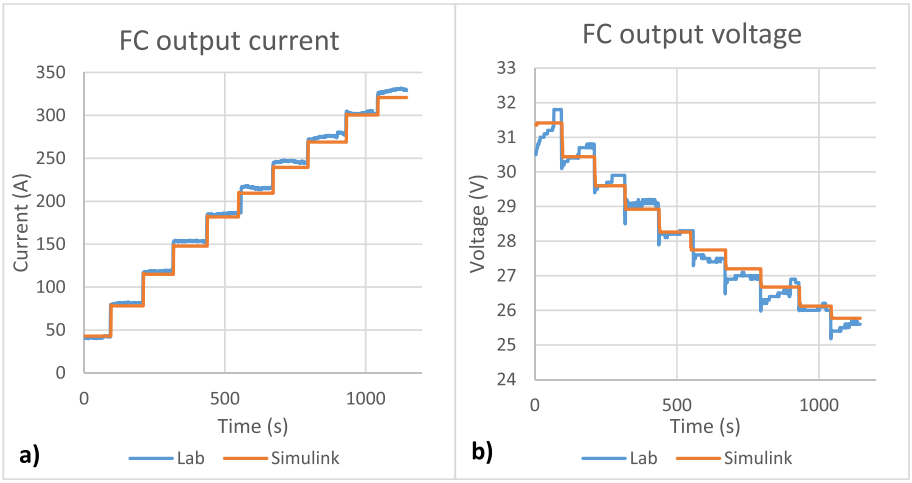

Fig. 2 – Validation of the Simulink FC model against practical results a) FC output current b) FC output voltage.

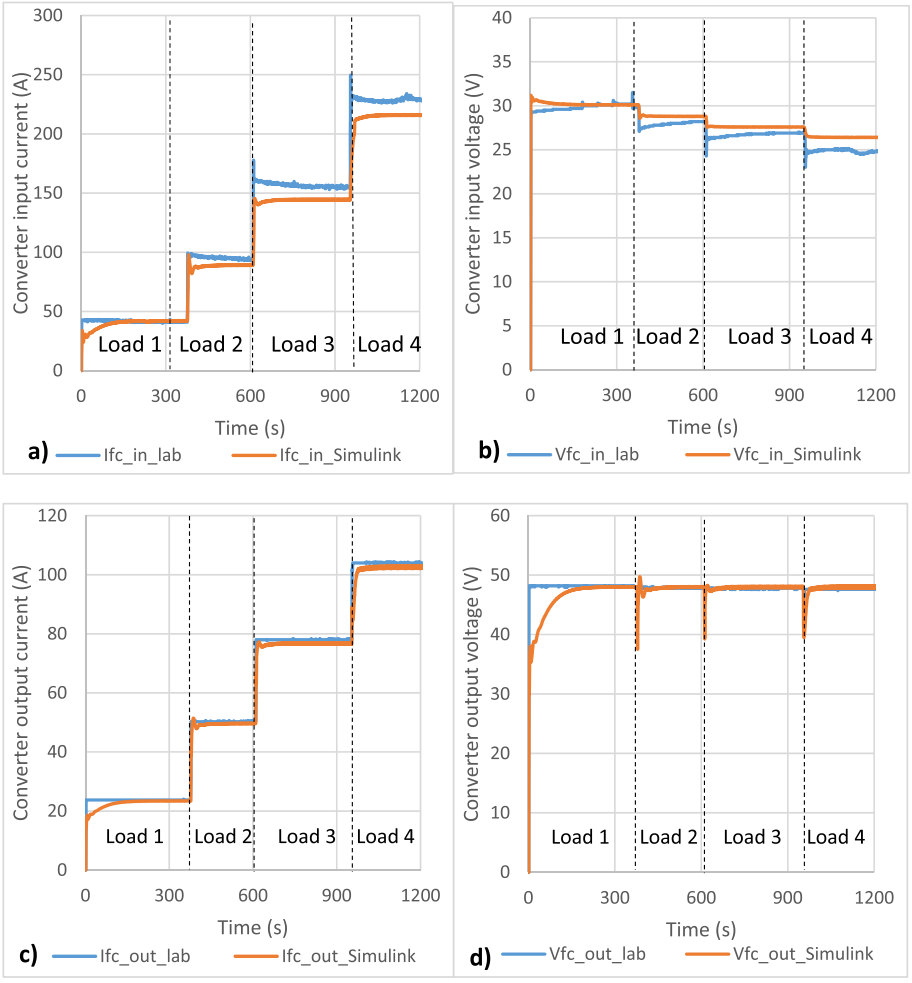

Fig. 3 – Validation of the Simulink FC and boost converter model against practical results a) Boost converter input current b) Boost converter input voltage c) Boost converter output current d) Boost converter output voltage.

short time to reset the new switching frequency to match the voltage change. Another reason is the logger sampling frequency of the laboratory system is lower than the Simulink model so not all transient responses may have been logged. Additionally, in the proposed FC/SC hybrid system, the FC is not expected to operate by responding directly to step changes in the power demand, so such voltage changes are not expected to occur.

Supercapacitor system validation

The SC system consists of a SC and a buck/boost converter. The SC selected for this FC hybrid model was the Maxwell 48 V Supercapacitor. In Simulink, a generic SC block can be parametrised to simulate a SC model. The generic SC model in Simulink utilises a controlled voltage source method. In this Simulink SC model, the SC output voltage is expressed using a Stern equation based on the SC specifications. The derivation of this equation is beyond the scope of this research and hence will not be discussed further. More details of the derivation of the Stern equation used in the Simulink model can be found in the literature [39–41].

A measure to control the charge and discharge would be required to validate the computer simulated SC model against the laboratory SC. A buck/boost converter was utilised to control the charge and discharge of the SC in the FC/SC hybrid drivetrain. An H bridge converter has been developed to control the output current of the buck/boost converter. Employing output current control means the buck/boost converter will control the current going in and out of the buck/boost converter (48 V bus bar side) to the load system. Charge and discharge tests were carried out to validate the computer model. In the discharge test, a 5 A user-defined discharge current (Isc_out)) was fed to a 10 Ω resistor. In the test, the SC started at 32 V initial voltage with this voltage boosted to 48 V by the converter, this leads to an output current 4.8 A at this resistive load. In the charge test, a constant 4.8 A current from an external 36 V source has been used to charge the SC. The aim is to use the controlled 4.8 A current to charge the SC from 0 V initial voltage to approximately 32 V. The discharge and charge tests have been carried out in both the computer model and laboratory system and compared in Fig. 4.

The comparison plots show the buck/boost converters of both the computer model and laboratory test rig capable of controlling the output current (Isc_out) at a user-defined 5 A. The main difference is the current has been limited to 30 A with the laboratory equipment for safety reasons while there is no need for a current limit for the Simulink buck/boost converter.

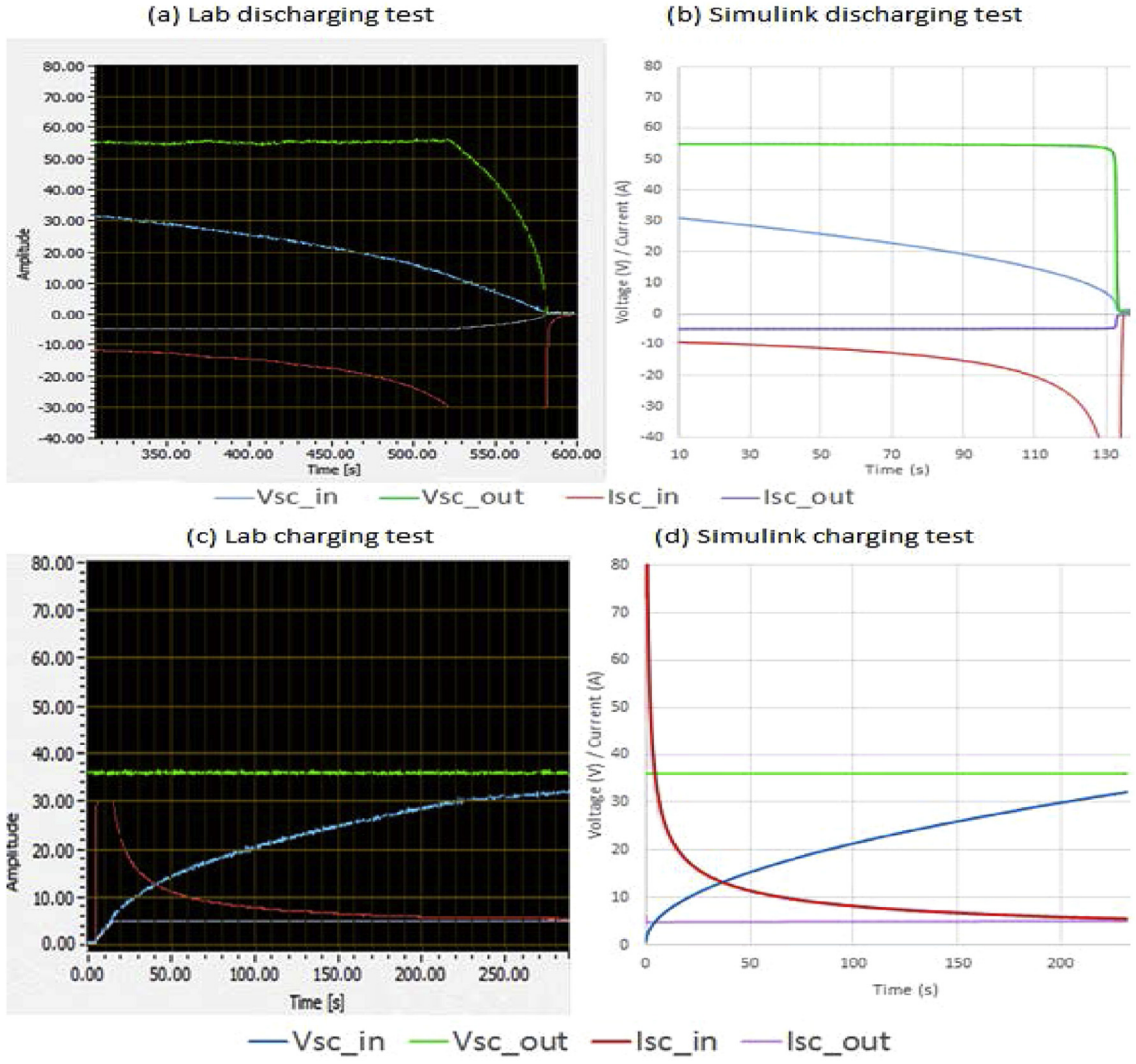

Fig. 4 – Validation of the Simulink SC and buck/boost converter model against practical results a) Laboratory discharge test b) Simulink discharge test c) Laboratory charge test d) Simulink charge test.

Load system simulation

The load system has been modelled using a variable resistor and a controlled source. The variable resistor will be switched on to dissipate the required amount of power to simulate motor mode while a controlled source will be switched on to provide the required power to simulate generator mode. Since the DC voltage in the hybrid system (downstream of the converters) is 48 V (regulated by the boost converter), the required power profile can be simulated by matching the current to and from the load. When the power is positive (powering the bus), the variable resistor will be switched on to dissipate the required amount of energy (power) calculated by:

$$R_{variable} = \frac{48^2}{P_{positive}} \quad (2)$$

When the power is negative (retarding the bus), the current source will be switched on to provide a controlled current. The current will be determined by:

$$I_{source} = \frac{P_{negative}}{48} \quad (3)$$

The system can determine the required resistance and current depending on the power requirement and by this means simulate the load on the FC/SC hybrid model. Although this is a different simulation method than that of the laboratory system, one of the important parameters of this research is to accurately represent the power profile required from or to the load. Not only can this load simulation method eliminate the requirement to simulate the motor/generator system, but also enable the simulation of more complex driving cycles which is a limitation of the equipment available in the laboratory test rig.

Integrated system

This section considers validation of the overall FC/SC hybrid system to ensure the computer model is representative of the laboratory system. A current control strategy focused on balancing the output current of the buck/boost converter was developed for the laboratory test rig and shown to be capable of maintaining control of the FC output [15]. The same current control strategy has also been integrated in the buck/boost converter model and the complete computer model has been shown in Fig. 5.

The model consists of a FC, boost converter, SC, buck/boost converter and load simulation system. The three parameters that the user is required to define are as follows.

1. FC and boost converter current output reference (slide: Ifc_ref value).
2. Driving cycle power profile (power_cycle from workspace block).
3. SC initial SoC (defined within the SC block).

System validation

The same experiments will also be carried out using both the laboratory test rig and computer model. The aim of which is the validation of the developed model and verify the performance of the control strategy. The experiments carried out for the laboratory test rig consists of a series of steady state and dynamic tests. The steady state tests were carried out to evaluate the fundamental operation of the control strategy under the three bus operating modes. The dynamic test was carried out to evaluate the control strategy under dynamic

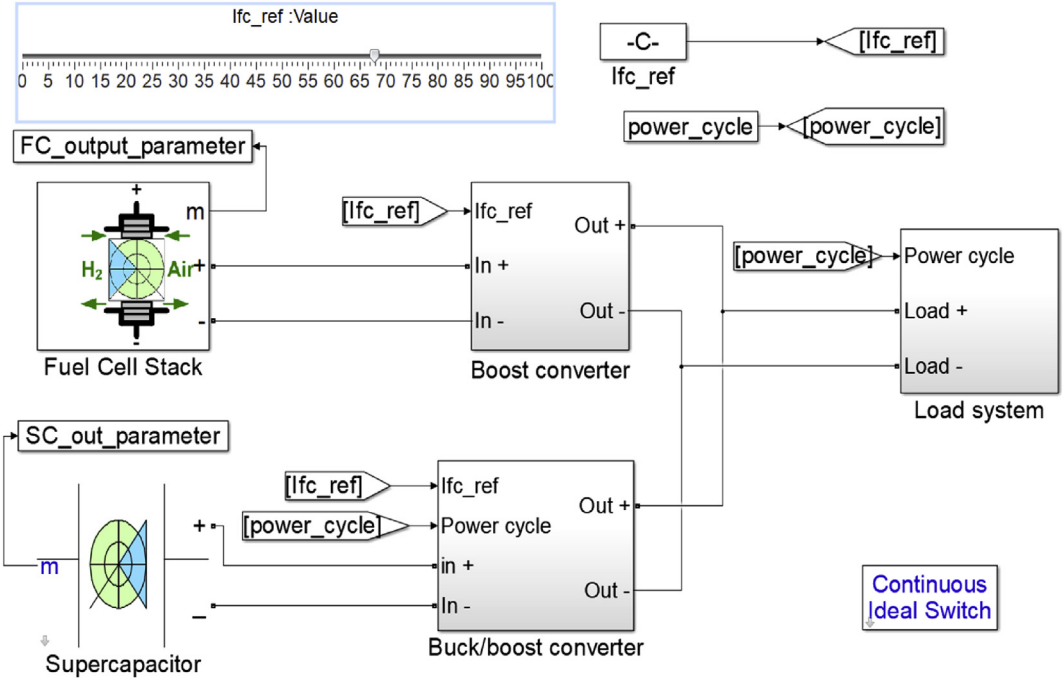

Fig. 5 – Simulink FC/SC hybrid model with controlling parameters.

Table 2 – Steady state test parameters for operating modes.

Parameter	Mode 1	Mode 2	Mode 3
FC and boost converter output current	40 A	80 A	10 A
SC and buck/boost converter output current	−40 A (discharge)	20 A (charge)	50 A (charge)
Load current	80 A	60 A	−40 A
FC and boost converter output power (Pfc_out)	1.92 kW	3.84 kW	0.48 kW
SC and buck/boost converter output power (Psc_out)	−1.92 kW	0.96 kW	2.4 kW
Load power (Pload)	3.84 kW	2.88 kW	−1.92 kW
Initial SoC	86%	26%	26%

loading, which, is more representative of a city driving bus under practical operating conditions. Details of the laboratory experiments can be found in Ref. [15].

Steady state test

A series of steady state tests were carried out to test the proposed control strategy operating in three different modes. In order to correctly validate the computational model, the same experimental environment was set up as for the experiments carried out with the laboratory test rig. The experimental parameters for the steady state tests are summarised in Table 2. The same parameters were used with the computer model. The results from the computer model have been compared against the results obtained from the laboratory test rig for validation.

The power balancing and SoC results for mode 1 operation are plotted in Fig. 6. The plotting parameters utilise the same parameter names as those in Table 2. In this experiment, the FC and boost converter provided a 1.92 kW output power and the SC and buck/boost converter also provided a 1.92 kW output power through discharge. The power from the FC and the SC have been combined to meet the 3.84 kW load power demand. This has been used to simulate bus operation there is a high transient power demand such as bus acceleration or ascending an incline. As can be seen from a comparison of the results in Fig. 6, the results from laboratory test rig and computer model are similar in terms of power balancing and SoC change. The final SoC of the mode 1 steady state test using the laboratory test rig is 36.9% while it is 35.3% for the computer model. The higher rates of oscillation evident in Fig. 6b) were a result of stray capacitance in the system. It should be noted that this will also be present in the laboratory system but is not visible due to the sampling period in the laboratory system (50 ms). The sampling frequency in the Simulink model was 1e-5 s and so was able to record the stray capacitance. Additionally, the load power in the laboratory test rig has been kept constant by manually adjusting the potentiometers. This result is the cause of the transient DC components seen in Figs. 6a, 7a and 8a.

The power balancing and SoC results for mode 2 operation are plotted in Fig. 7. In this experiment, the FC and boost converter provided a 3.84 kW output power while the load demand was 2.88 kW. As a result, the excess power of 0.96 kW has been used to charge the SC. This is expected to occur when the bus load is less than the power the FC and boost converter output provide. As the comparison results show, the power balancing and SoC results obtained from laboratory test rig and the computer model are similar. The final SoC for the laboratory test rig is 88.1% while it is 89.5% for the computer model.

The power balancing and SoC results for mode 3 operation are plotted in Fig. 8. In this experiment, the FC and boost converter output provides 0.48 kW output power while the load is providing a 1.92 kW power to the hybrid system. As such, the SC is being charged at a rate of 2.4 kW, which is the sum of the power from the FC and recovered energy from the load. This is only expected to occur when the bus engages regenerative braking. The computer model also produced similar results to those obtained from laboratory test rig. The final SoC of the laboratory test rig is 68.7% while it is 69.6% for the computer model.

The steady state tests show the computer model delivers performance results that are similar to those of the laboratory test rig for all three operating modes and validates the computer model under steady state working conditions. The power balancing shows near identical performance apart from some output trace oscillations and variations caused by equipment limitations within the laboratory test rig. The SoC throughout the three steady state tests showed slightly different results with an approximate 0.9–1.6% of difference in the final SoC being measured. This was a result of the difference in efficiencies between the DC/DC converters (both boost converter and buck/boost converter) of the laboratory test rig and the computer model. To investigate the efficiency difference, a series of additional steady state tests with different current ranges have been carried out for both the laboratory test rig and the computer model. The laboratory efficiency results were calculated based on results obtained from the laboratory test rig detailed in Ref. [15] while the Simulink efficiencies were calculated based on the results from the computer model. The efficiency results have been summarised in Table 3. As the results show, the difference in efficiencies measured between the laboratory test rig and the computer model varies from 1% to 7% dependent on the power range.

Dynamic test

The previous results validate the computer model under steady state conditions and show that the FC/SC hybrid system can operate as desired under steady state conditions. This section will deal with the application of dynamic loads to the computer model to validate the system under transient load conditions whilst maintaining the FC output steady.

The dynamic test aims to evaluate the system performance for a more complex driving cycle. The power profile for this test has to respond to and satisfy more frequent acceleration and deceleration points as frequent start, stop and speed changes are expected to occur during typical bus driving cycles. The FC and boost converter output reference were set to provide a constant 20 A output current, which equates to a 960 W power output, to evaluate the stabilised FC output

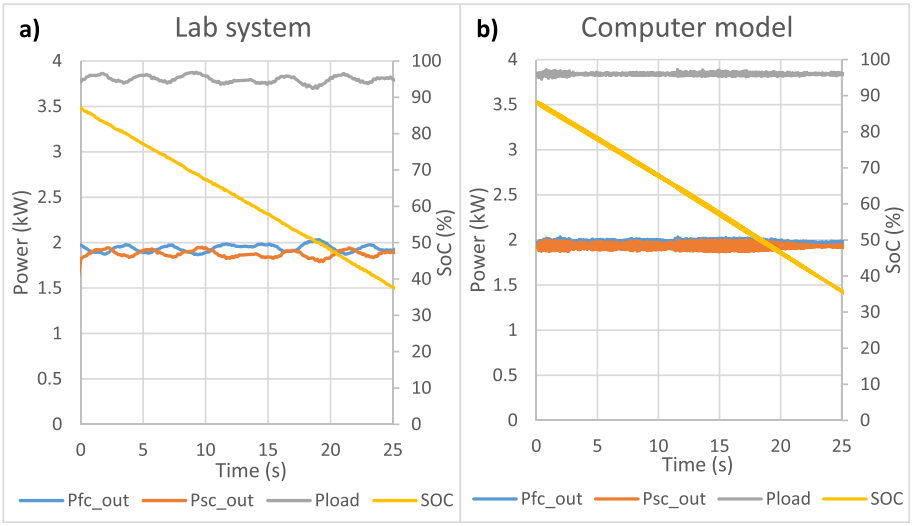

Fig. 6 – Steady-state performance with the FC and SC both providing power to meet the motor demand (mode 1 operation) a) Laboratory results b) Simulink simulation results.

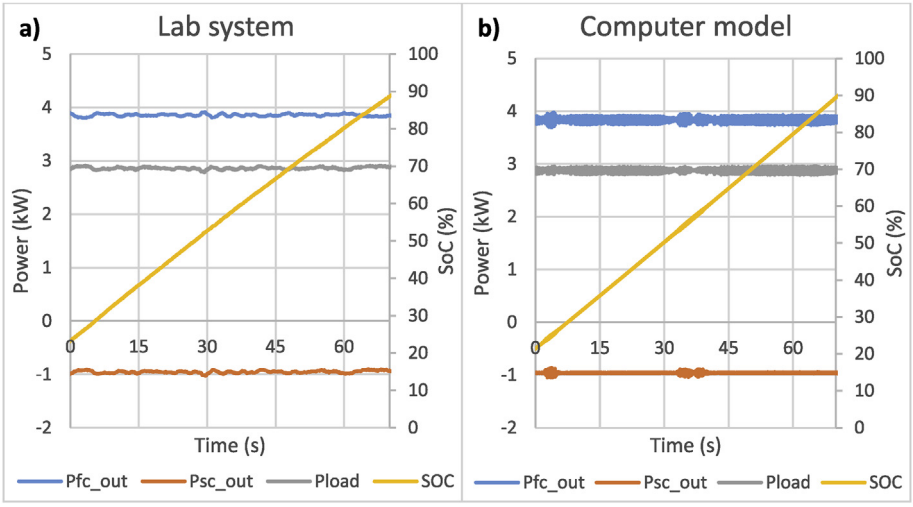

Fig. 7 – Steady-state performance with the FC providing for both the motor demand and SC charging (mode 2 operation) a) Laboratory results b) Simulink simulation results.

control strategy and validate the computer model. The same power profile was then applied to the computer model and the simulation results have been compared against the laboratory results. The power balancing results have been plotted in Fig. 9a and b. To better examine the validation, individual power parameter and the SoC changes have been compared in Fig. 10.

As can be seen from Fig. 9a and b, the load power is always the algebraic sum of the power from the FC (and boost converter) and the SC (and buck/boost converter). Fig. 10a, b and c showed the validation of individual power parameters. It can be seen in Fig. 10a that the power output of the FC generally remains stable for both the laboratory and Simulink simulation results. Some transient responses are seen in the Simulink results due to the discrete time-steps in the simulation and occur when the load power requirements transition from positive to negative. The FC and boost converter output for the laboratory system and computer model have both been kept at near 960 W, as was expected. There are two noticeable power drops as can be observed at 140 s and 204 s for the laboratory test rig and were caused by the 150 A current limit of the buck/boost converter which were discussed in detail in Ref. [15]. The regenerated power at these two points exceeded the 150 A current limit and hence forced the FC and boost converter output current to decrease. The decreased FC and boost converter output also reduced the charging power to the SC and buck/boost converter, thus the charging power at those two points were less than at the corresponding points with the computer model. The current safety limit is not a problem for the computer model. As a result, and despite the oscillations, the FC and boost converter output power in the computer model were kept reasonably constant.

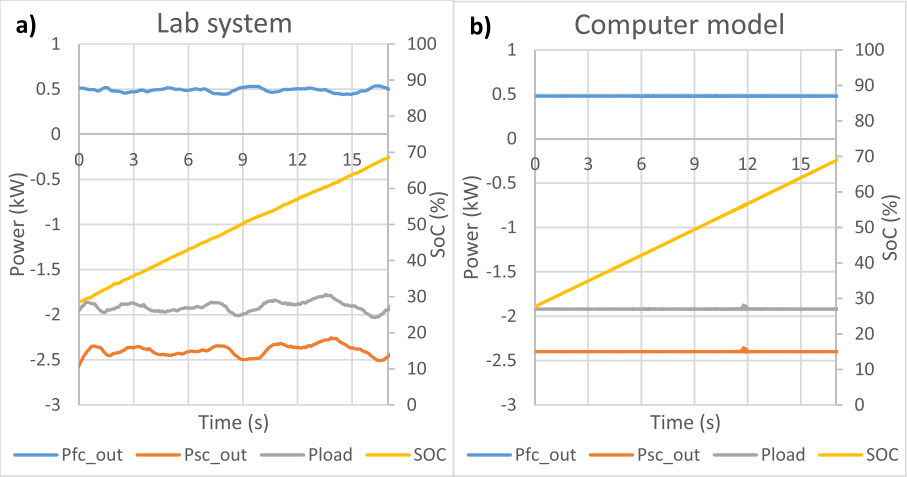

Fig. 8 – Steady-state operation with both the FC and motor regenerative power charging the SC (mode 3 operation) a) Laboratory results b) Simulink simulation results.

Table 3 – Steady state test efficiency comparison between laboratory test rig and computer model.

Average Boost converter efficiency			Average buck/boost converter efficiency (charge)			Average buck/boost converter efficiency (discharge)		
Ifc_ out	Lab	Simulink	Isc_ Out	Lab	Simulink	Isc_ out	Lab	Simulink
10	0.8795	0.8760	10	0.9032	0.9577	10	0.9866	0.9372
20	0.9135	0.8713	20	0.9222	0.9671	15	0.9919	0.9494
30	0.9185	0.8564	30	0.9358	0.9864	20	0.9888	0.9492
40	0.9229	0.8412	40	0.9234	0.9709	30	0.9881	0.9395
50	0.9080	0.8415	50	0.9418	0.9885	35	0.9813	0.9444
60	0.9043	0.8350	60	0.9277	0.9765	40	0.9674	0.9439
70	0.8967	0.8349	80	0.9235	0.9836	50	0.9499	0.9240
80	0.8840	0.8351	100	0.9039	0.9811	55	0.9496	0.9345
90	0.8841	0.8338				60	0.9352	0.9130
						70	0.8787	0.9173
						75	0.8945	0.9371

For the SoC comparison shown in Fig. 10d, the SoC curve from the computer model is generally 1–2% lower than that for the laboratory test rig. The final SoC from the laboratory test rig is 75.6% and 74.4% for the computer model. There are two main reasons for this SoC difference. The first is the converter efficiency difference as stated earlier. The second is the safety requirement to limit the circuit current when using the laboratory test rig, so the SoC comparison results show a difference in performance, particularly at times when the system current is close to the 150 A limit.

Table 4 gives an example of energy balance for the dynamic test for both the Simulink model and laboratory test bench. The cumulative energy has been calculated by multiplying the real time power by each sampling time. It can be seen that the energy delivered to the load is the sum of the energy from the FC and the SC. The negative SC cumulative energy indicates the SC has been charged after the dynamic test, hence a higher final SoC then the initial SoC. The energy balance showed the Simulink model has reasonable close performance (<3% difference) to the laboratory test bench as well. The dynamic test demonstrated that the proposed control strategy is capable of operating satisfactorily within a transient driving cycle while meeting the requirement to maintain the FC output constant and controlled. Although there are some relatively minor differences caused by converter efficiency differences and the current safety limitation, the results from the computer model and system performance closely match those from the laboratory test rig.

Full scale FC/SC hybrid model

Up to this point, this paper has detailed the development of a computerised representation of a scaled FC/SC hybrid system and control strategy and its comparative performance against a laboratory test rig FC/SC scale system. As discussed before, the computer model can enable much easier component modification than the laboratory system. Since the computer model has been shown to be representative of the laboratory system, the computer model can now be used for further investigation. The laboratory test rig, against which the Simulink computer model was validated, is a ten percent scale representation of a practical FC/SC bus. In the following section, the validated computer model will be scaled up to enable

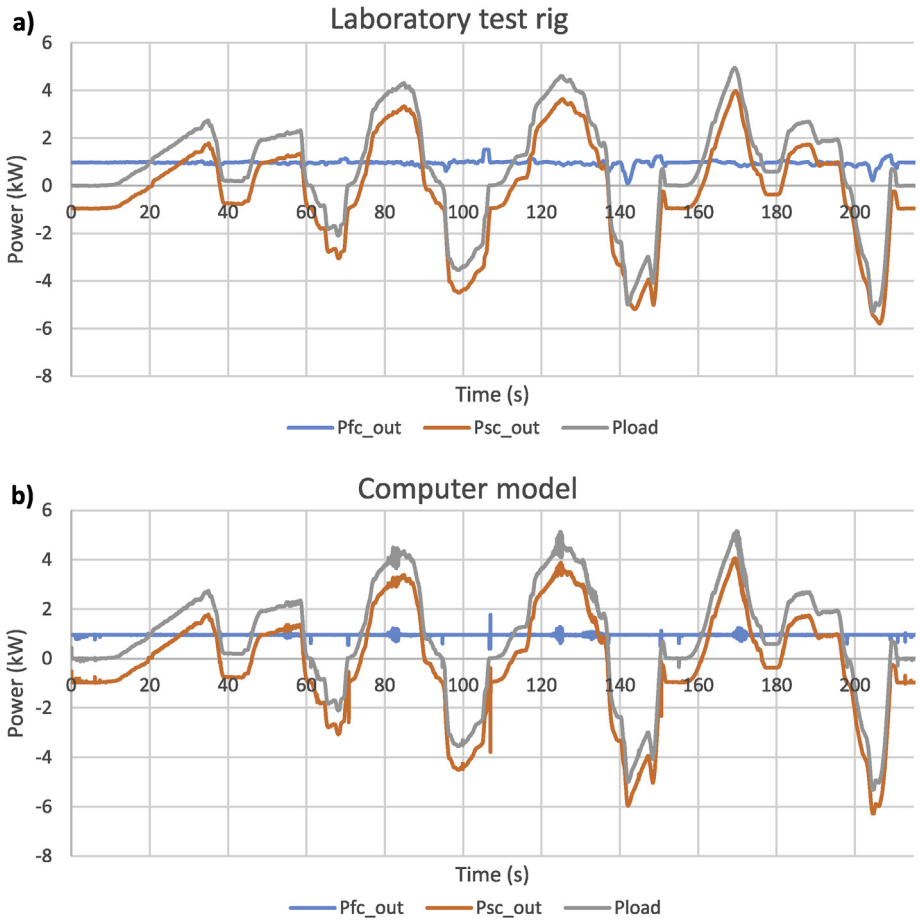

Fig. 9 – Power balancing for the dynamic test a) Laboratory results b) Simulink simulation results.

analysis of the performance and control strategy of the hybrid FC/SC power unit against load profiles representative of a full sized bus. There are three main components that require parameter scaling to model the power requirements of a full scale bus. These are the FC (as the primary power source), the SC (as the energy storage system) and the busbar voltage (to match and satisfy the requirement of the propulsion motor and control system). The scaling of the system primarily focussed on the rated power of each of the components.

The FC used in the scaled laboratory test rig was an 8.5 kW PEMFC. The computerised full scale FC was selected to represent a Ballard FCvelocity 85 kW PEMFC which is an off the shelf FC used for transportation applications. The 85 kW FC can be simulated in Simulink based on the manufacture's specifications [42]. The 85 kW FC has an operating output voltage range of 280–420 V.

The 48 V SC module used in the laboratory test rig and scaled computer model has been scaled up to a rated voltage of 480 V. To create a representative simulation of the laboratory system, the SC must have an energy storage capacity of 10 times that used in the laboratory system. This is because the charge and discharge power of the SC needs to be 10 times larger in the full scale simulation than that in the laboratory system. To achieve this, ten of the modules used for the laboratory test rig would be connected in series for the up scaled computer model to provide the desired voltage and energy storage capacity. As a result of series connection, the energy capacity of this module can be determined as:

$$Stored\ energy = 0.5 \times 8.3F \times 480^2 \div 3600s = 0.2656\ kWh$$

Another consideration for the SC module is the maximum deliverable power. SCs have excellent power density characteristics. The SC module used in the laboratory test rig has a maximum power output of 56 kW (1150 A). Since the full scale system model has the ten modules connected in series, the maximum output current would still be 1150 A. However, the rated voltage of the modules would increase to 480 V, giving a peak power output of 560 kW. In contrast a parallel connection of the SC modules would increase the peak current whilst maintaining the SC system output voltage at 48 V. Either way the maximum power output of the SC will scale with the number of modules whether they are connected in series or parallel. Regardless of the configuration of the ten SCs, the overall SC power rating will be sufficient for the power requirements of bus transport applications.

The scale model hybrid system utilised 48 V as the busbar voltage as a safety requirement of the laboratory test rig. This voltage level is too low to power a practical bus system. Since 630 V is a common busbar voltage for diesel electric hybrid buses, the same busbar voltage will be used for the full scale computerised bus model. This would allow known motor parametric and performance data to be used for the FC bus

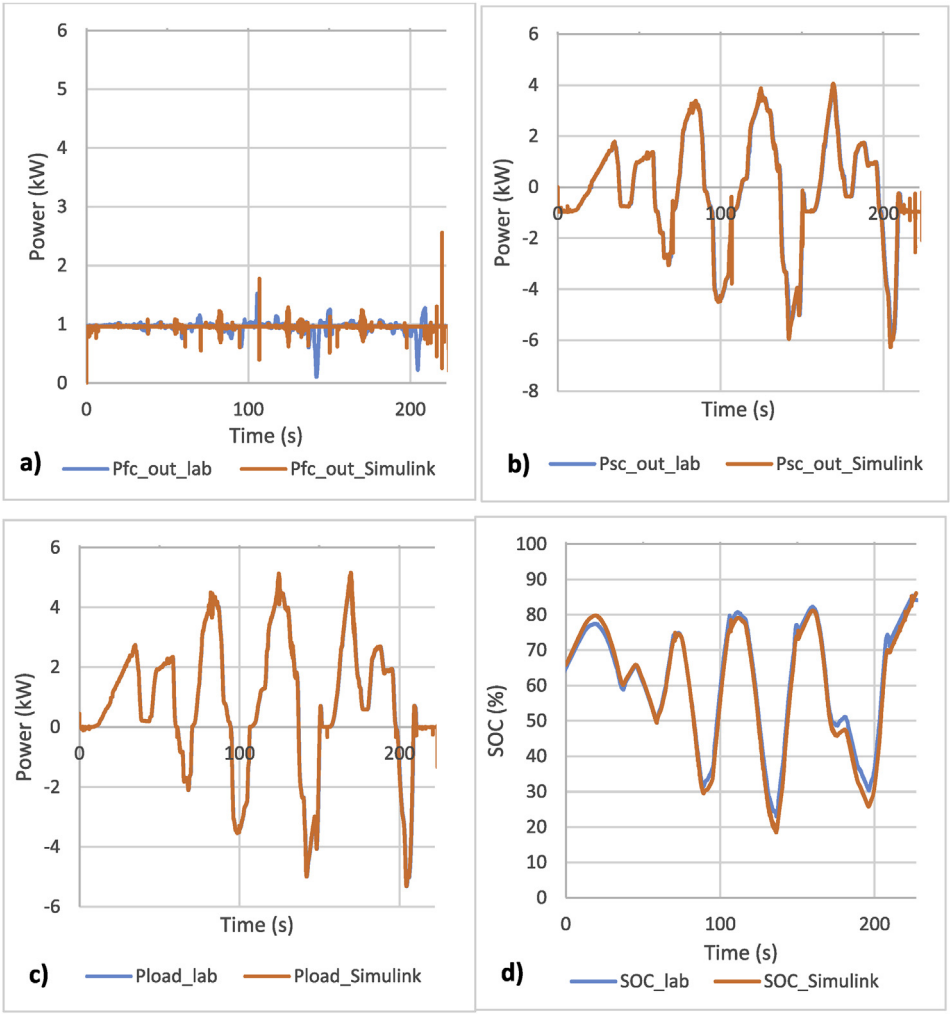

Fig. 10 – Individual parameter validation for the dynamic test a) Pfc_out b) Psc_out c) Pload d) SoC.

which would significantly reduce simulation set up time. The boost converter for the full scale 85 kW FC has therefore been scaled to produce a 630 V output. A summary of scaling information of the laboratory test rig and scaled up computer model has been provided in Table 5.

The full scale model has been evaluated with the dynamic test to investigate the performance of the proposed control strategy at full scale power levels. The load profile in the dynamic test has also been scaled up to be ten times that of the profile used in the scaled model. Although the increased busbar voltage of 630 V will decrease the current, the focus of the scaling is to balance the power using the proposed control algorithm. The same control strategy has been applied to the

Table 4 – Energy balance in the FC hybrid system for the dynamic test.

Energy	Laboratory	Simulink
Cumulative energy delivered by the FC after boost converter	212,640 J	217,215 J
Cumulative energy delivered by the SC after buck/boost converter	- 49,016 J	−48,591 J
Cumulative energy delivered to the load (include regenerative energy)	164,146 J	168,836 J
Cumulative regenerative energy received	−115,521 J	−116,091 J

Table 5 – Scale and full scale FC/SC hybrid model specification.

	Scale	Full scale
PEMFC		
Model	Hydrogenics HD8	Ballard FCvelocity
Rated power	8.5 kW	85 kW
Operating current	0–380 A	0–288 A
Operating voltage	20–40 V	280–420 V
SC		
Model	Maxwell P048 B01	Maxwell P048 B01
Number of SC unit	1	10
Total capacitance	83 F	8.3 F
Rated voltage	48 V	480 V
Stored energy	0.0265 kWh	0.265 kWh
Hybrid system		
Bus bar voltage	48 V	630 V

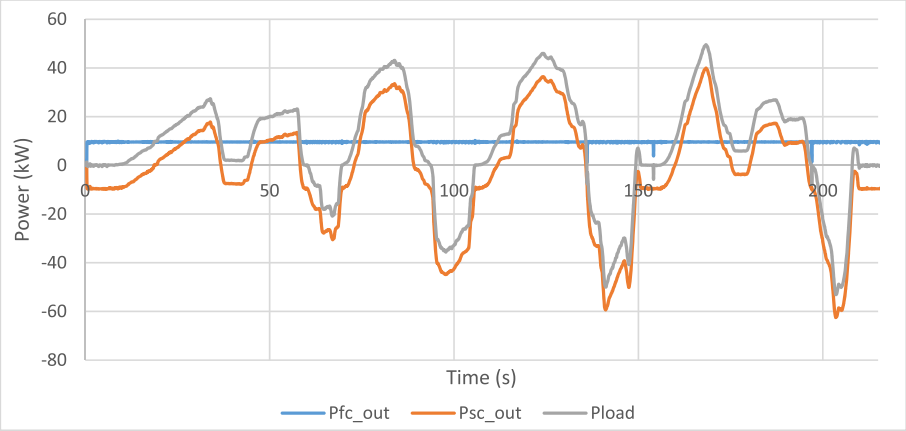

Fig. 11 – Power balancing for the dynamic test with full scale model.

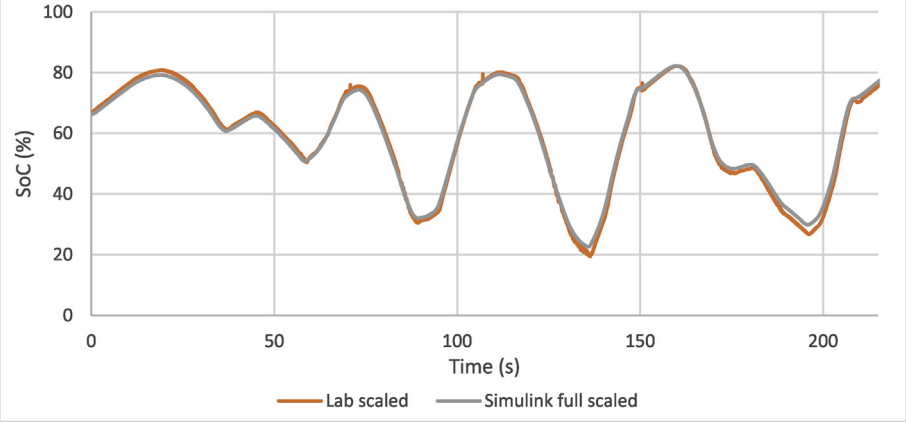

Fig. 12 – SoC comparison for dynamic test between the laboratory test rig and the full scale Simulink model.

full scale model and the results, in terms of power balancing of the hybrid system has been plotted in Fig. 11.

As Fig. 11 shows, the FC and boost converter power has been kept at a near constant 9.6 kW (15.2 A* 630 V) which is ten times that of the 960 W (20 A*48 V) power used in the scale model. Since the SC size and power profile has been increased by the same magnitude, the SoC change between the laboratory scaled system and the Simulink full scale model have also been compared and plotted in Fig. 12.

As Fig. 12 shows, the SoC of both systems closely follow the same trend with some minor differences (<1.5%) which are deemed to be within acceptable limits. These differences are mainly caused by the efficiency differences in the converters. It can be seen that the power balancing operated as expected with the full scale model and the stabilised FC output control strategy also works at the power levels of a practical bus.

Conclusion

This research provides guidance for FC/SC hybrid bus design from a power system engineering point of view. The research investigated the use of FCs hybridised with SCs for city bus use. The proposed FC/SC control strategy focused on keeping the FC output constant while using the SC to supplement the dynamic load demands. To conduct research into this field, a scaled FC hybrid system aimed at investigating the proposed control strategy has been developed as both a computer model and a laboratory test rig. The computer model was validated at both the individual component levels and as an integrated hybrid system. The validated scaled FC/SC hybrid model showed the control strategy functioned as expected in terms of keeping the FC output constant and user controlled. The hybrid controller, for controlling the power flows, has also been tested and showed good capability in managing the power balance between the FC and the SC power sources. Both steady state tests and dynamic tests have demonstrated the proposed control strategy functioned to satisfy the overall load while maintaining the FC output constant with both the laboratory system and computer model. Limitations of the model have also been addressed. It was concluded that each model is suitable for use in this research and capable of accurately representing practical FC and SC systems. The validated computer model can be used as a tool to carry out further FC hybrid system performance evaluation, system configuration modification and enabling more accessible system optimisation. Finally, the computer model has been scaled up to be representative of a full sized bus in terms of power output and control and demonstrated the control strategy mimicked that of the laboratory test rig as did the

computer scale model. This would enable practical driving cycles to be evaluated with the full scale computer model as part of future work to further investigate the potential of the proposed stabilised control strategy.

Acknowledgement

This material is based on work supported by the Engineering and Physical Sciences Research Council (EPSRC), HyFCap Project under grant EP/K021192/1. The authors would also like to thank Mr Konrad Yearwood for his input and advice relating to this work.

REFERENCES

[1] DEFRA. Air pollution in the UK 2013. 2014.
[2] TfL. Transport emissions Roadmap. 2014.
[3] RACF. Air quality and road transport impacts and solutions. 2014.
[4] CIWEM. Clearing the air priorities for reducing air pollution in the UK. 2013.
[5] Howard R, Beevers S, Dajnak D, The Capital City Foundation (set up by Policy Exchange), King's College London. Up in the air, how to solve London's air quality crisis: part 2. 2016.
[6] TfL. Health, safety and environment report 2014/15. 2015.
[7] Li JQ. Battery-electric transit bus developments and operations: a review. Int J Sustain Transp 2016;10:157–69. https://doi.org/10.1080/15568318.2013.872737.
[8] Carroll S. Green fleet technology study for public transport. 2015.
[9] Coyle F. London buses emissions reduction, vol. 15; 2014.
[10] Chong U, Yim SHL, Barrett SRH, Boies AM. Air quality and climate impacts of alternative bus technologies in greater London. Environ Sci Technol 2014;48:4613–22. https://doi.org/10.1021/es4055274.
[11] Gregory D, Mclaughlin O, Mullerder S, Sundararajah N. New solutions to air pollution challenges in the UK. Imperial College London and The Grantham Institute; 2016.
[12] O'Hayre R, Cha S-W, Colella W, Prinz FB. Fuel cell fundamentals. Hoboken, NJ, USA: John Wiley & Sons, Inc; 2016. https://doi.org/10.1002/9781119191766.
[13] Partridge J, Wu W, Bucknall R. Development of bus drive technology towards zero emissions: a review. Hybrid Electr Veh 2017. https://doi.org/10.5772/68139.
[14] Element Energy Limited. Post-2014 London hydrogen activity: options assessment. 2012.
[15] Wu W, Partridge JS, Bucknall RWG. Stabilised control strategy for PEM fuel cell and supercapacitor propulsion system for a city bus. Int J Hydrogen Energy 2018;43:12302–13.
[16] Wu W, Partridge JS, Bucknall RWG. Development and modelling of a lab scaled PEM fuel cell drive system for city driving application. In: UPEC, Coimbra, Port. Sept. 6-9th 2016; 2016.
[17] Venkateshkumar M, Raghavan R, Kumarappan N. Design of a new multilevel inverter standalone hybrid PV/FC power system. Fuel Cell 2015;15:862–75. https://doi.org/10.1002/fuce.201400085.
[18] Shin D, Lee K, Chang N. Fuel economy analysis of fuel cell and supercapacitor hybrid systems. Int J Hydrogen Energy 2016;41:1381–90. https://doi.org/10.1016/j.ijhydene.2015.10.103.
[19] Papra M, Büchi FN, Kötz R. Investigating the dynamics of a direct parallel combination of supercapacitors and polymer electrolyte fuel cells. Fuel Cell 2010;10:873–8. https://doi.org/10.1002/fuce.200900197.
[20] Wu B. MAP. Design and testing of a 9.5kW proton exchange membrane fuel cell supercapacitor passive hybrid system. Int J Hydrogen Energy 2014;39:7885.
[21] Silva RE, Harel F, Jemeï S, Gouriveau R, Hissel D, Boulon L, et al. Proton exchange membrane fuel cell operation and degradation in short-circuit. Fuel Cell 2014;14:894–905. https://doi.org/10.1002/fuce.201300216.
[22] Kuo JK, Hsieh HK. Research of flywheel system energy harvesting technology for fuel cell hybrid vehicles. Fuel Cell 2013;13:1234–41. https://doi.org/10.1002/fuce.201300129.
[23] Garcia P, Fernández LM, Garcia CA, Jurado F. Comparative study of PEM fuel cell models for integration in propulsion systems of urban public transport. Fuel Cell 2010;10:1024–39. https://doi.org/10.1002/fuce.201000002.
[24] Martín IS, Ursúa A, Sanchis P. Modelling of PEM fuel cell performance: steady-state and dynamic experimental validation. Energies 2014;7:670–700. https://doi.org/10.3390/en7020670.
[25] Pei P, Yuan X, Gou J, Li P. Dynamic response during PEM fuel cell loading-up. Mater (Basel) 2009;2:734–48. https://doi.org/10.3390/ma2030734.
[26] Azib T, Larouci C, Chaibet A, Boukhnifer M. Online energy management strategy of a hybrid fuel cell/battery/ultracapacitor vehicular power system. IEEJ Trans Electr Electron Eng 2014;9:548–54. https://doi.org/10.1002/tee.22004.
[27] De Luca D, Fragiacomo P, De Lorenzo G, Czarnetski WT, Schneider W. Strategies for dimensioning two-wheeled fuel cell hybrid electric vehicles using numerical analysis software. Fuel Cell 2016;16:628–39. https://doi.org/10.1002/fuce.201500174.
[28] Meyer RT, DeCarlo RA, Meckl PH, Doktorcik C, Pekarek S. Hybrid model predictive power management of A fuel cell-battery vehicle. Asian J Contr 2013;15:363–79. https://doi.org/10.1002/asjc.553.
[29] Zhao H, Burke AF. Fuel cell powered vehicles using supercapacitors-device characteristics, control strategies, and simulation results. Fuel Cell 2010;10:879–96. https://doi.org/10.1002/fuce.200900214.
[30] Yulianto A, Simic M, Taylor D, Trivailo P. Modelling of full electric and hybrid electric fuel cells buses. Procedia Comput. Sci 2017;112:1916–25. https://doi.org/10.1016/j.procs.2017.08.036. Elsevier B.V.
[31] Behdani A, Naseh MR. Power management and nonlinear control of a fuel cell e supercapacitor hybrid automotive vehicle with working condition algorithm. Int J Hydrogen Energy 2017;42:24347–57. https://doi.org/10.1016/j.ijhydene.2017.07.197.
[32] Melo P, Ribau J, Silva C. Urban bus fleet conversion to hybrid fuel cell optimal powertrains. Procedia – Soc Behav Sci 2014;111:692–701. https://doi.org/10.1016/j.sbspro.2014.01.103.
[33] Fares D, Chedid R, Karaki S, Jabr R. Optimal power allocation for a FCHV based on linear programming and PID controller. Int J Hydrogen Energy 2014;39:21724–38. https://doi.org/10.1016/j.ijhydene.2014.09.020.
[34] Li T, Liu H, Zhao D, Wang L. Design and analysis of a fuel cell supercapacitor hybrid construction vehicle. Int J Hydrogen Energy 2016;41:12307–19. https://doi.org/10.1016/j.ijhydene.2016.05.040.
[35] Zheng CH, Oh CE, Park YI, Cha SW. Fuel economy evaluation of fuel cell hybrid vehicles based on equivalent fuel consumption. Int J Hydrogen Energy 2012;37:1790–6. https://doi.org/10.1016/j.ijhydene.2011.09.147.

[36] Odeim F, Roes J, Wülbeck L, Heinzel A. Power management optimization of fuel cell/battery hybrid vehicles with experimental validation. J Power Sources 2014;252:333–43. https://doi.org/10.1016/j.jpowsour.2013.12.012.
[37] Fletcher T, Thring R, Watkinson M. An Energy Management Strategy to concurrently optimise fuel consumption & PEM fuel cell lifetime in a hybrid vehicle. Int J Hydrogen Energy 2016;41:21503–15. https://doi.org/10.1016/j.ijhydene.2016.08.157.
[38] Hydrogenics. Fuel Cell power systems. 2018. http://www.hydrogenics.com/hydrogen-products-solutions/. [Accessed 23 February 2018].
[39] Drummond R, Howey DA, Duncan SR. Low-order mathematical modelling of electric double layer supercapacitors using spectral methods, vol. 3. Univ Oxford; 2014. https://doi.org/10.1016/j.jpowsour.2014.11.116.
[40] Balakrishnan A, Subramanian K. Nanostructured ceramic oxides for supercapacitor applications. CRC press Tylor & Francis group; 2014. https://doi.org/10.1201/b16522.
[41] Wu D. Control of a super-capacitor based energy storage system. Univ Manchester; 2013. p. 176.
[42] Ballard. FCveloCity® motive module product portfolio. 2018. http://ballard.com/fuel-cell-power-products/motive-modules. [Accessed 21 February 2018].